

EXPERIMENTAL STUDY ON COHERENCE STRUCTURE IN THE NEUTRAL ATMOSPHERIC SURFACE LAYER WITH A LARGER-SCALE DISTURBANCE

Yasuo Hattori

Fluid Dynamics Sector,
Central Research Institute of Electric Power Industry (CRIEPI)
1646 Abiko, Abiko-shi, Chiba 270-1194, Japan
yhattori@criepi.denken.or.jp

Chin-Hoh Moeng

Mesoscale & Microscale Meteorology Division,
National Center of Atmospheric Research (NCAR)
3450 Mitchell Lane, Boulder, Colorado 80307-3000, U.S.A
moeng@ucar.edu

Hitoshi Suto

Fluid Dynamics Sector,
Central Research Institute of Electric Power Industry (CRIEPI)
1646 Abiko, Abiko-shi, Chiba 270-1194, Japan
suto@criepi.denken.or.jp

Hiromaru Hirakuchi

Fluid Dynamics Sector,
Central Research Institute of Electric Power Industry (CRIEPI)
1646 Abiko, Abiko-shi, Chiba 270-1194, Japan
hiromaru@criepi.denken.or.jp

Nobukazu Tanaka

Fluid Dynamics Sector,
Central Research Institute of Electric Power Industry (CRIEPI)
1646 Abiko, Abiko-shi, Chiba 270-1194, Japan
n-takana@criepi.denken.or.jp

ABSTRACT

A wind-tunnel experiment was carried out to understand the vertical coherence structures in the near-neutral surface layer under the influences of a larger-scale disturbance, which often exists in the atmosphere. A fully developed logarithmic layer along a surface, which mimicked the atmospheric surface layer with a larger-scale disturbance was examined. The disturbance with a scale larger than that of boundary layer shear turbulence was generated by using an active grid. The 2-dimensional velocity vectors in the streamwise-vertical plane were measured with a PIV technique. The large-scale fluid motions extracted with a proper orthogonal decomposition showed various flow patterns, such as an irrotational fluid motion and a swirling flow, caused by the larger-scale disturbance. The scale of these fluid motions corresponded to the logarithmic layer height. The existence of a layered structure in the logarithmic layer was also revealed, i.e., the velocity fluctuation in a streamwise direction was mainly generated in a lower layer, whereas vertical fluid motions frequently appeared in an upper layer.

Such fluid motions in an upper layer cause the increase in vertical-velocity fluctuations and the deviation from the Monin-Obhkhof theory.

INTRODUCTION

An accurate description of turbulence statistics, including higher-order moments, in the neutral atmospheric surface layer, is of practical interest in the wind-resistance design for structures (e.g. Zhou et al., 2002; IEC ed., 2003; Ishikawa, 2004). The turbulence statistics in the surface layer has been commonly estimated by Monin-Obhkhof theory. However, recent observations (Högström, 1990; Högström et al., 2002; Drobinski et al., 2004; 2007) indicate that such statistics are often inconsistent with this theory under the neutral conditions; e.g. the observed turbulence intensity of vertical-velocity fluctuation is not constant in the surface layer, as predicted by the theory, but varies with height.

To firmly grasp why such violation from the theory occurs, coherence structures in the surface layer have been also investigated with the helps of rapid distortion theory and large eddy simulations (Högström et al., 2002; Carlotti and Drobinski 2004; Foster et al., 2006; Drobinski et al., 2007). These studies suggest that effects of larger-scale disturbances on the surface layer are essential to the peculiar turbulence characteristics; larger-scale disturbances, which often exist in the atmosphere, might produce vertical eddy motions in the surface layer and change the vertical turbulence transport non-locally.

However, the details of spatial structure, especially vertical coherent structure, have not been clarified yet, because of the difficulty in obtaining multi-point simultaneous velocities in observations and the limitation of spatial resolution near the surface of numerical simulations under high Re number conditions. Indeed, two eddy-motion models, which oppose each other, have been proposed for explaining the vertical coherence structure in the neutral surface layer under the influences of larger-scale disturbances, i.e., one is based on “top-down (detached)” eddy motions (e.g. Högström et al., 2002; Drobinski et al., 2007), and the other is based on “bottom-up (attached)” eddy motions (e.g., Hommema and Adrian 2003; Macnaughton, 2004). Thus, the controversy over the nature of coherence structure in the near-surface atmospheric boundary layer has continued.

On the other hand, we have recently attempted to mimic such atmospheric surface layer in a test section of a wind tunnel (Hattori et al., 2009). The disturbance in the test section was generated with an active grid devised by Makita et al. (1987), and the scale of disturbance was much larger than that of boundary layer shear turbulence. Then, we confirmed that the turbulence statistics in the logarithmic layer of the fully developed boundary layer along a smooth flat surface in the test section are consistent with those of observations in the near-neutral atmospheric surface layer with the adjustment in the movement of active grid, implying that this experiment is useful to examine the turbulence characteristics in the surface layer.

The purpose of present study is to clarify the vertical structure in the logarithmic layer under the influences of the larger-scale disturbance. We have carried out the wind-tunnel experiment with the active grid, and examined velocity vectors fields in the fully-developed logarithmic layer. The two-component velocity vectors in a streamwise -vertical plane were measured with a PIV technique, and fluid motions in a vertical plane were discussed with a proper orthogonal decomposition (POD) in details.

EXPERIMENTAL APPARATUS AND PROCEDURE

The experiments were conducted in the CRIEPI wind tunnel (Hattori et al., 2000; Hattori, 2001). A schematic drawing of the wind tunnel is shown in Fig. 1. The test section is $1,000 \times 1,000 \text{ mm}^2$ in area and 6,200 mm long. The larger-scale disturbance, the scale of which is much larger than that of boundary layer shear turbulence, was generated by an active grid devised by Makita et al. (1987). This grid has been widely used to study isotropic turbulence of high Reynolds number flows (e.g., Mydlarski and Warhaft 1996; Poorte and Biesheuvel 2002; Kang et al., 2003; Savelsberg and Water 2008) and to control the

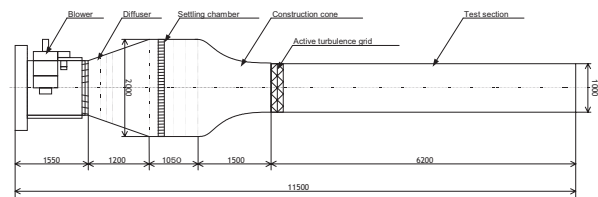


Fig. 1 Schematic drawing of wind tunnel

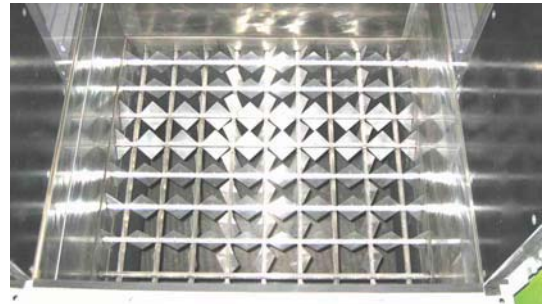


Fig. 2 Photograph of active turbulence grid in test section of wind tunnel

turbulence statistics in a boundary layer (e.g. Sekishita et al., 2002; Larssen, 2005; Yue et al., 2008). Here, we used it to generate a larger-scale disturbance to simulate turbulence characteristics in the neutral-surface layer. Figure 2 presents the photograph of our active turbulence grid, which was installed at the front of the test section. The design follows those of previous studies, composing of rotating grid bars with attached triangular agitator wings, stepping motors located at the end of each grid bars outside the wind tunnel, and a controller. The mesh spacing M , between the grid bars, was 110 mm, providing a tunnel cross-section of $10M \times 10M$. Each of the 18 grid bars with triangular wings independently rotated and flapped in a random way with a stepping motor, and this movement was controlled by a program on PC.

The 2-components velocity vectors in the streamwise-vertical (x - z) plane were measured with a PIV technique. Olive-oil mist added to the boundary layer were illuminated by light sheet discharged from a double pulse Nd:YAG laser (90mJ/pulse) system. Particle-containing flow images with a physical size of $88.4 \times 88.4 \text{ mm}^2$ were captured by a CCD camera ($2,048 \times 2,048$ pixels). This physical size corresponds to the logarithmic layer height, and thus no larger-scale structure, the scale of which is much larger than logarithmic layer height, is observed in this measurement. The velocity vectors were calculated using a cross-correlation method with interrogation windows of a size of 64×64 pixels. The overlap ratio was 50 %, and the 4,096 velocity vectors were obtained in each pair of images.

The freestream velocity was 5.0 ms^{-1} , and the measuring location was fixed at the distance $x=4,180 \text{ mm}$ ($x/M = 38$) downstream from the active grid where turbulence was fully developed and the measured vertical profiles of turbulence statistics, including higher-order moments, and the power spectra of fluctuating velocity near the surface, agreed well with those of observations (Hattori et al., 2009). As

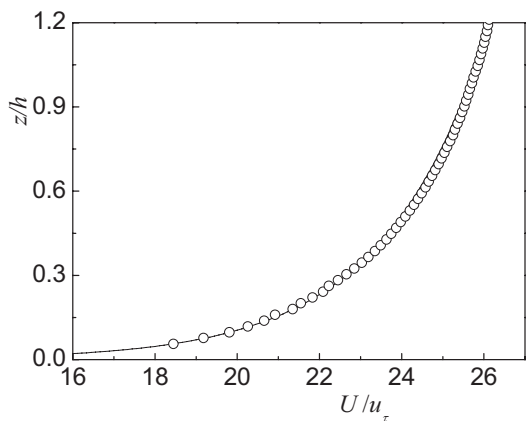


Fig. 3 Vertical profile of streamwise mean velocity; solid line is for $U/u_\tau = 5.76 \log(z/2.6 \times 10^{-6})$.

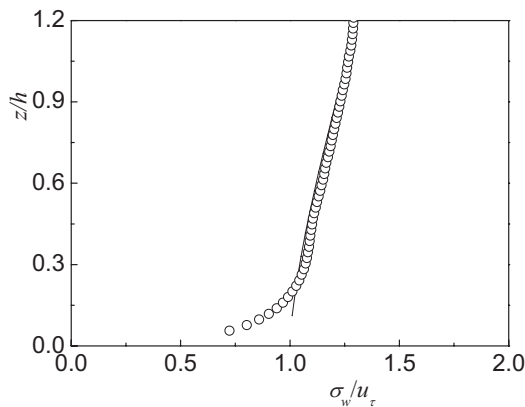


Fig. 4 Vertical profiles of turbulence intensity of vertical-velocity fluctuation; solid line is for $(\sigma_w/u_\tau)^2 = 1 + [z/(0.67h)]^{2/3}$.

examples, the vertical profiles of streamwise mean velocity U and turbulence intensity of vertical-velocity fluctuations σ_w , which are measured with a PIV technique in the present study, are shown in Figs. 3 and 4, respectively. The statistics are estimated with 1,200 snapshots velocity vectors and the profiles are normalized with the friction velocity $u_\tau (= 0.2 \text{ ms}^{-1})$ and the logarithmic layer height $h (= 6.7 \text{ mm})$. For $z/h < 1$ (in the logarithmic layer), the profile of U and σ_w are adequately represented by the logarithmic law: $U/u_\tau = 5.76 \log(z/2.6 \times 10^{-6})$, and the relationship: $(\sigma_w/u_\tau)^2 = 1 + [z/(0.67h)]^{2/3}$. These normalized profiles agree well with those of observations (Högström et al., 2002; Drobinski et al., 2007).

RESULTS AND DISCUSSION

To properly capture the dynamics of large-scale fluid motions, we use a proper orthogonal decomposition (POD) method based on snapshots (instantaneous velocity vector fields) (Adrian et al., 2000; Meyer et al., 2007). In this analysis, velocity vector fields in a plane were expanded in POD modes with expansion coefficients. The total kinetic

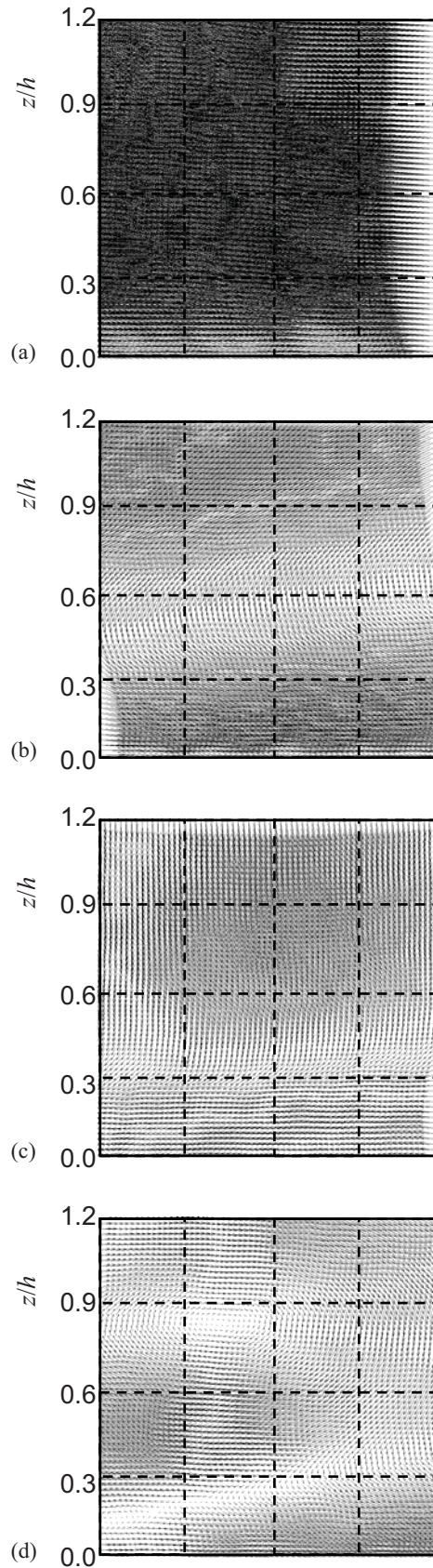


Fig. 5 Velocity fluctuation vectors with POD eigenmodes; (a)-(d) are for POD mode 1 – 4, respectively.

energy from velocity fluctuations in the snapshots that is associated with a given POD-mode is proportional to the corresponding eigenvalue. Thus, we can observe the energetic and hence largest structures of the velocity fluctuation in the low modes of POD. In the present study, 1,200 snapshots taken in the same vertical plane are used to perform the POD analysis. To examine the dependence on the number of snapshots, the analysis has been repeated with only 300 snapshots. The results agreed qualitatively with the results with 1,200 snapshots, but there were somewhat different quantitatively. The accuracy of the POD based on 1,200 snapshots is therefore found to be satisfactory for the present study, the purpose of which is to clarify the structural characteristics of large-scale fluid motions.

The velocity fluctuation vectors for four most energetic POD modes are shown in Fig. 5. The coordinates are normalized with the logarithmic layer height h ($= 6.7$ mm), and to ease comparison between different modes, the same scaling of velocity vectors has been used for plots of velocity vectors. Note that the POD modes must be multiplied by its corresponding POD-coefficient to represent real fluctuation vectors, and thus the sign and the length of the vectors do not have physical meaning until combined with the coefficients used in reconstruction of snapshots. As shown in the figures, the flow pattern in the logarithmic layer changes with POD modes. The POD modes 1 and 2 show an irrotational fluid motion and a swirling flow in the whole logarithmic layer, respectively. The POD mode 3 clearly shows the layer structure with the border of layers located at $z/h = 0.3$, i.e., the fluid motions with streamwise-velocity fluctuations are dominant in a lower layer ($z/h < 0.3$), whereas the velocity fluctuations in a streamwise direction almost disappear and those only in a vertical direction are generated in an upper layer ($z/h > 0.3$). The fluctuation velocity vectors field of mode 4 is similar to those of low modes for a logarithmic layer without larger-scale disturbances (Adrian et al., 2000). This implies that the flow patterns with the POD mode 1, 2 and 3 are due to the larger-scale disturbance.

The contributions of these flow patterns of the POD mode 1, 2 and 3 to the turbulence intensities of velocity fluctuations were then investigated. The vertical profiles of turbulence intensities of the reconstructed velocity fluctuations with POD modes 1, 2 and 3 are shown in Figs. 6 and 7. These statistics are normalized with the values of the reconstructed velocity fluctuations with all POD modes. The streamwise-velocity fluctuations, σ_u , are mainly generated by the POD mode 1, i.e., the velocity fluctuations of mode 1 represents almost of intensity (over 50 %). This indicates that the velocity fluctuations in a streamwise direction are closely related to the irrotational fluid motion. The contributions of low POD modes to the vertical-velocity fluctuations, σ_w , are significantly small compared with σ_u . The intensity of POD mode 1 is under 20% of total POD modes. With the addition of POD mode 2, the intensity increases in the whole logarithmic layer, but that value remains a small (about 30 %). The POD mode 3 is significantly stronger than the remaining modes in the upper layer ($z/h > 0.3$), whereas its contribution to the intensity is almost zero in the lower layer ($z/h < 0.3$).

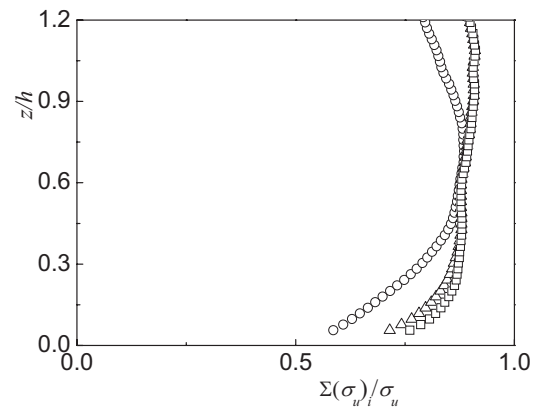


Fig. 6 Vertical profiles of turbulence intensity of streamwise-velocity fluctuation with POD modes; circles are for POD mode 1, triangles are for POD mode 1 and 2, squares are for POD mode 1-3.

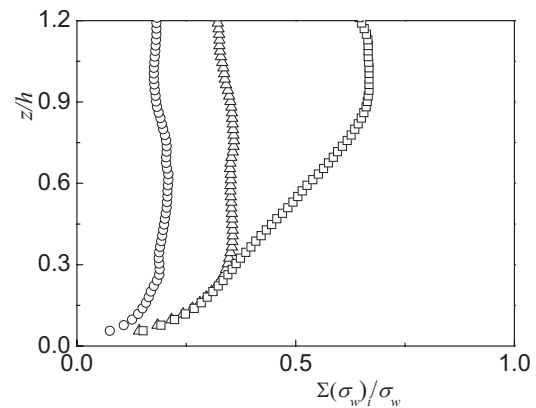


Fig. 7 Vertical profiles of turbulence intensity of vertical-velocity fluctuation with POD modes; circles are for POD mode 1, triangles are for POD mode 1 and 2, squares are for POD mode 1-3.

From these results, we found that the larger-scale disturbance affects the vertical structures in the logarithmic layer and generates peculiar flow patterns, such as an irrotational fluid motion and a swirling flow. In particular, the fluid motion of POD mode 3 clearly shows the layered structure. The layered structures have been observed in the near-neutral atmospheric surface layer (Drobinski et al., 2004; 2007). Högström et al. (2002) also predicted the existence of a layered structure through the analysis with a rapid distortion theory, and thus, our experimental results might correspond to such observations.

Figs 5 and 7 suggested that the vertical-velocity fluctuation are mainly generated by the layered flow motions (POD mode 3), and such fluid motions cause the increase in σ_w with the height. To understand the origin of the increase in σ_w with the height might be a key of the effects of larger-scale disturbance, because Monin-Obkhof theory predicts the homogeneous intensity in the surface layer. Figure 8 demonstrates a typical low- and high-pass filtered instantaneous velocity vectors reconstructed with the POD modes. The snapshot has been selected by looking

for snapshots where only mode 3 has a large coefficient, while the rest of the first few coefficients take values relatively close to zero. This selects a snapshot where the POD mode 3 can be seen in a “clean” form. The low-pass filtered velocity vectors clearly shows the impingement flow onto the surface in the upper layer ($z/h > 0.3$), and such a flow causes active vortex motions in the lower layer ($z/h < 0.3$) as shown in high-pass filtered velocity vectors. This snapshot might represent ‘top down’ fluid motion in the surface layer proposed by Högström et al. (2002).

CONCLUDING REMARKS

To understand the structural characteristics in the near-neutral atmospheric surface layer with the larger-scale disturbance, we carried out a wind-tunnel experiment. A larger-scale disturbance in the test section was generated by an active grid. With this disturbance a fully developed logarithmic layer mimicked the atmospheric surface layer was obtained. The 2-dimensional velocity vectors in the streamwise-vertical plane were measured with a PIV technique, and the large-scale fluid motions were extracted with a proper orthogonal decomposition (POD). The fluctuation velocity vectors of low POD modes, which are directly associated with large-scale fluid motions, showed various flow patterns, such as an irrotational fluid motion, a swirling, with a large scale, which corresponds to the logarithmic layer height. A layered structure, the boundary of which was near the surface was also observed. Fluid motions in an upper layer caused the increase in intensity of vertical-velocity fluctuations, suggesting that such flow was one of the origins of the deviation from the Monin-Obkhof theory.

The authors would like to thank Dr. Sun, Juan Zhen and Dr. Soichiro Sugimoto for helps of the collaboration between NCAR and CRIEPI and Mr. Takayuki Mizuno for helps of the wind-tunnel experiments. C.-H. Moeng’s work is supported by the National Center for Atmospheric Research, USA, which is sponsored by the National Science Foundation.

REFERENCES

- Adrian, R. J., Christensen, K.T., and Liu, Z.-C., 2000, “Analysis and interpretation of instantaneous turbulent velocity fields,” *Exp. in Fluids*, vol. 29, pp.275-290.
- Carlotti, P., and Drobninski, P., 2004, “Length scales in wall- bounded high-Reynolds-number turbulence,” *J. Fluid. Mech.*, vol. 516, pp. 239-264.
- Drobninski, P., Carlotti, P., Newsom, R.K., Banta, R.M., Foster, R.C., and Redelsperger, J.-L., 2004, “The structure of the near-neutral atmospheric surface layer,” *J. Atmos. Sci.*, vol. 61, pp. 699-713.
- Drobninski P, Carlotti P, Redelsperger J-L, Banta RM, Masson V, Newsom R (2007) “Numerical and experimental investigation of the neutral atmospheric surface layer,” *J. Atmos. Sci.*, vol. 64, pp. 137-156.
- Foster, R.C., Vianey, F., Drbinski, P., and Carlotti, P., 2006, “Near-surface coherent structures and the vertical momentum flux in a large-eddy simulation of the neutrally-

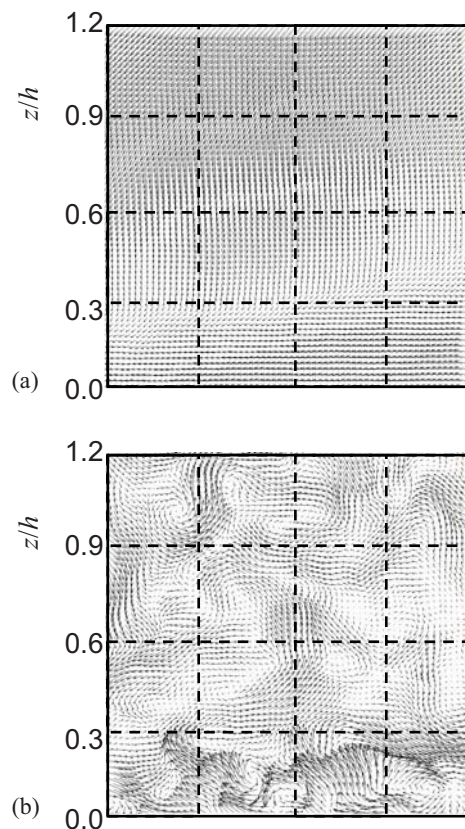


Fig. 8 Typical low- and high-pass filtered instantaneous velocity vectors with POD modes; (a) is for low-pass filtered vectors and (b) is high-pass filtered vectors.

stratified boundary layer,” *Boundary-Layer Meteorology*, vol. 120, pp. 229-255.

Hattori, Y., Tsuji, T., Nagano Y., and Tanaka, N., 2000, “Characteristics of turbulent combined-convection boundary layer along a vertical heated plate,” *Int. J. Heat Fluid Flow*, vol. 21, pp. 520-525.

Hattori, Y., 2001, “Turbulent characteristics and transition behavior of combined-convection boundary layer along a vertical heated plate,” ph.D thesis, Nagoya Institute of Technology.

Hattori, Y., Moeng, C.-H., Suto, H., Hirakuchi, H., and Tanaka, N., 2009, “Wind-tunnel experiment on the neutral atmospheric surface layer with larger-scale disturbance,” *Boundary-Layer Meteorology*, (submitted).

Högström, U., 1990, “Analysis of turbulence structure in the surface layer with a modified similarity formulation for near neutral conditions,” *J. Atmos. Sci.*, Vol. 47, pp. 1949-1972.

Högström, U., Hunt, J.C.R., and Smedman A.-S., 2002 “Theory and measurements for turbulence spectra and variances in the atmospheric neutral surface layer,” *Boundary-Layer Meteorology*, vol. 103, pp. 101-124.

Hommema, S., and Adrian, R.J., 2003, “Packet structure of surface eddies in the atmospheric boundary layer,” *Boundary-Layer Meteorology*, vol. 106, pp. 147-170.

International Electrotechnical Commission, 2005, “IEC 61400-1 ed. 3, Wind turbines-part1: design requirements”.

Ishikawa, T., 2004, "A study on wind load estimation method considering dynamic effect for overhead transmission lines," ph.D thesis, Waseda University.

Kang, H. S., Chester, S., and Meneveau, C., 2003, "Decaying turbulence in an active-grid- generated flow and comparisons with large-eddy simulation," *J. Fluid Mech.* Vol. 480, pp. 129-160.

Larssen, J.V., 2005, "Large scale homogeneous turbulence and interactions with a flat-plate cascade," ph.D thesis, Virginia polytechnic institute and state University.

Makita, H., Sassa, K., Iwasaki, T., and Iida, A., 1987, "Evaluation of the characteristics features of a large-scale turbulence field (1st report, performance of the turbulence generator," *Trans. JSME (B)*, vol. 53, pp. 3173-3186 (*in Japanese*).

Menaughton, K.G., 2004, "Attached eddies and production spectra in the atmospheric logarithmic layer," *Boundary-Layer Meteorology*, vol. 111, pp. 1-18.

Meyer, K. E., Pedersen, J. M., and Özcan, O., 2007, "A turbulent jet in crossflow analysed with proper orthogonal decomposition," *J. Fluid Mech.*, vol.583, pp.199-227.

Mydlarski, L., and Warhaft, Z., 1996, "On the onset of high-Reynolds-number grid-generated wind tunnel turbulence," *J. Fluid Mech.*, vol. 320, pp. 331-368.

Poorte, R.E.G., and Biesheuvel, A., 2002, "Experiments on the motion of gas bubbles in turbulence generated by an active grid," *J. Fluid. Mech.*, vol. 461, pp. 127-154.

Savelsberg, R., and Water, W., 2008, "Turbulence of a free surface," *Physical review letters.*, Doi: 10.1103/PhysRevlett.100.034501.

Sekisita, N., Makita, H., Ichigo, M., and Fujita, T., 2002, "Simulation of atmospheric turbulent boundary layer in a wind tunnel," *Trans. JSME(B)*, vol. 68, pp. 55-62 (*in Japanese*).

Yue, W., Meneveau, C., Parlange, M.B., Zhu, W., Kang, H.S., and Katz, J., 2008, "Turbulent kinetic energy budgets in a model canopy: comparisons between LES and wind-tunnel experiments," *Environ. Fluid Mech.*, vol. 8, pp. 73-95.

Zhou, Y., Kijewsk, T., and Kareem, A., 2002, "Along-wind load effects on tall buildings: comparative study of major international codes and standards," *J. Structural Eng.*, vol. 126, pp. 788-796.